A Fourth-Order Central Runge-Kutta Scheme for Hyperbolic Conservation Laws

Mehdi Dehghan, Rooholah Jazlanian
Department of Applied Mathematics, Faculty of Mathematics and Computer Science, Amirkabir University of Technology, Tehran, Iran

Received 5 February 2009; accepted 12 July 2009
Published online 27 October 2009 in Wiley Online Library (wileyonlinelibrary.com).
DOI 10.1002/num.20530

In this work, a new formulation for a central scheme recently introduced by A. A. I. Peer et al. is performed. It is based on the staggered grids. For this work, first a time discritization is carried out, followed by the space discritization. Spatial accuracy is obtained using a piecewise cubic polynomial and fourth-order numerical derivatives. Time accuracy is obtained applying a Runge-Kutta(RK) scheme. The scheme proposed in this work has a simpler structure than the central scheme developed in (Peer et al., Appl Numer Math 58 (2008), 674–688). Several standard one-dimensional test cases are used to verify high-order accuracy, nonoscillatory behavior, and good resolution properties for smooth and discontinuous solutions. © 2009 Wiley Periodicals, Inc. Numer Methods Partial Differential Eq 26: 1675–1692, 2010

Keywords: central Runge-Kutta(CRK) scheme; central scheme; hyperbolic conservation laws; nonlinear limiters; nonoscillatory scheme; weighted essentially nonoscillatory (WENO) technique

I. INTRODUCTION

Hyperbolic systems of conservation laws arise in many practical problems such as biological models [1], shallow water flow [2], discrete kinetic models [3], magnetohydrodynamic (MHD) [4], and many other areas in science and engineering [5, 6]. Analytical solutions are available only in very few special cases. Therefore, the numerical solution of hyperbolic systems of conservation laws has been an important field of research for the last decades.

The schemes more commonly used in context are the so-called shock capturing schemes(see, for example, the book by LeVeque [7]). Among shock capturing schemes, the most commonly used are finite volume schemes. For these schemes, the conservation laws are integrated in space and time on control volumes. Therefore, the equation is transformed in integral form. In this formulation, to update the solution and the cell averages, it is necessary to evaluate numerical intermediate values of the quadrature formula and flux functions at the edge of each cell.

The necessity of high accuracy and sharp resolution of the discontinuities motivated the development of high order techniques for conservation laws, for example, see [8–10]. Most

Correspondence to: Mehdi Dehghan, Department of Applied Mathematics, Faculty of Mathematics and Computer Science, Amirkabir University of Technology, Tehran, Iran (e-mail: mdehghan@aut.ac.ir)

high order shock capturing schemes are obtained in conservative form. Then the conservation properties of the systems of hyperbolic conservation laws are automatically satisfied. These schemes are based on three main ingredients. The main ingredients are the non-oscillatory reconstruction, a suitable numerical flux function, and, of course, a suitable discretization in time.

Among finite volume methods, one should distinguish between upwind and central schemes. It is known that a scheme is upwind if it makes extensive use of the characteristic information of the system, while a scheme is central if characteristic information is not used. In this work, we are interested in central scheme such as black-box, Jacobian-free solvers, that is, a scheme which requires little knowledge about the eigenstructure of the system of conservation laws.

The prototype of upwind schemes is first order upwind, which is first order Godunov method [11], based on the solution of the Riemann problem at cell edges. The prototype of central schemes is first order Lax-Friedrichs (LxF) scheme [12]. Like the Godunov method, it is based on piecewise constant approximate solution and unlike the Godunov method, the LxF scheme is Riemann-solver-free.

Generally, upwind schemes gain sharper resolution than central schemes for the same order of accuracy and spatial grids because they require some knowledge about the eigenstructure, but are more expensive, and are more complicated to be implemented. For this reason, in recent years, central schemes got considerable attention.

A second-order central procedure was proposed by Nessyahu and Tadmor (NT) [9]. The NT scheme is based on the reconstruction of piecewise linear polynomial from the known cell-averages. Because the NT scheme is Riemann-solver-free, so it is simple to be implemented. Also this scheme was extended to multidimensional problems [13].

A third-order central scheme was proposed by Liu and Tadmor [8]. This method is based on the nonoscillatory third-order reconstruction of Liu and Osher [14]. This scheme has a major advantage of the central schemes over the upwind schemes, in that no Riemann solvers are involved. The central schemes have been implemented successfully in many areas, such as semiconductor modeling [15], kinetic models [16], extended thermodynamics [16, 17], and Hamilton-Jacobi equation [18].

Central Runge-Kutta(CRK) schemes are another approach for solving hyperbolic conservation laws. These methods were proposed by Pareschi, Puppo, and Russo [19].

In this work, we present a new fourth-order CRK scheme based on staggered grids. For this, we use the reconstruction of Peer et al. [10] and Runge-Kutta scheme of fourth-order. The new scheme is obtained starting from the equation for the evolution of cell averages on staggered cells. The new formulation obtained in this article has a simpler structure than the previous central scheme based on staggered grids [10]. It should be noted that in this new formulation it is not necessary to use quadrature formula (Simpson's rule) for the fluxes function which in turn implied the evaluation of Natural Continuous Extension (NCE) of Runge-Kutta (RK) scheme [20]. Then it requires a smaller number of evaluations per time step, therefore, the new scheme is more efficient than the previous central scheme.

This article is organized as follows. In Section II we give a brief review of Godunov-type methods (central and upwind schemes) for one-dimensional hyperbolic conservation laws, and in Section III, we describe the new formulation of fourth-order central Runge-Kutta (CRK) scheme. A linear stability analysis of the new scheme is carried out in Section IV. In Section V, we report the numerical results computed using the new technique. Finally, Section VI ends this article with a brief summary.

II. REVIEW OF GODUNOV-TYPE METHODS

We are interested in computing approximate solutions to the hyperbolic systems of conservation laws

$$u_t + f(u)_x = 0, \tag{1}$$

with $u \in \mathbb{R}^m$, $f : \mathbb{R}^m \to \mathbb{R}^m$ is continuously differentiable subject to the initial condition $u(x,0) = u_0(x)$.

We will denote by I_x the cell centered around the point x, that is, $I_x = [x - \frac{h}{2}, x + \frac{h}{2}]$. Also let Δt be the mesh width in time, that is, $\Delta t = t^{n+1} - t^n$ and u_j^n is used for $u(x_j, t^n)$. Introduce the cell averages of u on $I_j := I_{x_j}$ and $I_{j+\frac{1}{2}} := I_{x_{j+\frac{1}{2}}}$ at time t^n

$$\bar{u}_j^n = \frac{1}{h}\int_{I_j} u(x,t^n)dx, \quad \bar{u}_{j+\frac{1}{2}}^n = \frac{1}{h}\int_{I_{j+\frac{1}{2}}} u(x,t^n)dx.$$

Integrating (1) over I_x, we obtain

$$\frac{d\bar{u}}{dt}|_x = -\frac{1}{h}\left[f\left(u\left(x+\frac{h}{2},t\right)\right) - f\left(u\left(x-\frac{h}{2},t\right)\right)\right]. \tag{2}$$

Here $\frac{d\bar{u}}{dt}|_x = \frac{1}{h}\int_{I_x} u_t(\xi,t)d\xi$. So far, Eq (2) is exact and gives the evolution in time of the cell averages. Finite volume schemes are based on the discretization of (2) in time. Once one has a semidiscrete evolution equation for the cell average, as (2), one needs a numerical ODE solver, rather than a quadrature formula. Starting from the old cell averages $\{\bar{u}^n\}$ at time t^n, we look for the cell averages at next time step t^{n+1}. A key point in both upwind and central schemes is the reconstruction step. From the cell averages $\{\bar{u}^n\}$, it is necessary to reconstruct the initial data $w(x,t^n) \sim u(x,t^n)$, that is,

$$w(x,t^n) = P_j^n(x), \quad x_{j-\frac{1}{2}} < x < x_{j+\frac{1}{2}},$$

where $P_j^n(x)$ should be conservative, with r as order of accuracy, and non-oscillatory. The reconstruction in general will be discontinuous at the end points of the interval I_j. Now, integrating (2) over $[t^n, t^{n+1}]$, we obtain

$$\bar{u}^{n+1}(x) = \bar{u}^n(x) - \frac{1}{h}\int_{t^n}^{t^{n+1}}\left[f\left(u\left(x+\frac{h}{2},t\right)\right) - f\left(u\left(x-\frac{h}{2},t\right)\right)\right]dt. \tag{3}$$

As is said in [21], the choice of $x = x_j$ in (3) results in an upwind scheme. The solution then may be nonsmooth in the neighborhood of the points $\{x_{j+\frac{1}{2}}\}$, and the evaluation of the flux integrals in (3) requires the use of a computationally expensive (approximate) Riemann solver and characteristic decomposition. If $x = x_{j+\frac{1}{2}}$ in (3), we obtain central techniques, namely

$$\bar{w}_{j+\frac{1}{2}}^{n+1} = \frac{1}{h}\int_{I_{j+\frac{1}{2}}} w(x,t^n)dx - \frac{1}{h}\left[\int_{t^n}^{t^{n+1}} f(w(x_{j+1},t))dt - \int_{t^n}^{t^{n+1}} f(w(x_j,t))dt\right]. \tag{4}$$

In contrast to the upwind method, the solution is smooth in the neighborhood of the points $\{x_j\}$. Then, we can use an appropriate quadrature formula for the time integrals in (4). The intermediate

values of the quadrature formula can be computed either by Taylor expansion [8] or by Natural Continuous Extension (NCE) of the Runge-Kutta scheme [22].

The staggered cell averages $\bar{w}^n_{j+\frac{1}{2}}$ which are used on the right hand side of (4) are given by

$$\bar{w}^n_{j+\frac{1}{2}} = \frac{1}{h}\int_{I_{j+\frac{1}{2}}} w(x,t^n)dx = \frac{1}{h}\left[\int_{x_j}^{x_{j+\frac{1}{2}}} P^n_j(x)dx + \int_{x_{j+\frac{1}{2}}}^{x_{j+1}} P^n_{j+1}(x)dx\right].$$

III. DESCRIPTION OF THE FOURTH-ORDER CRK SCHEME

Before describing a new fourth-order Central Runge-Kutta scheme, we shall briefly describe a suitable notation for Runge-Kutta schemes applied to the initial value problems. Let us consider

$$\begin{cases} y' = F(y(t)), \\ y(t_0) = y_0. \end{cases}$$

The solution obtained at time t^{n+1} with a $\nu-$step explicit RK method of order p can be written as

$$y^{n+1} = y^n + \Delta t \sum_{i=1}^{\nu} b_i K^{(i)},$$

where the $K^{(i)}$'s are the RK fluxes

$$K^{(i)} = F\left(y^n + \Delta t \sum_{j=1}^{i} a_{ij} K^{(j)}\right), \quad i = 1, \ldots, \nu.$$

The matrix $A = (a_{ij})$, and the vector b define uniquely the RK scheme. With the present notation, A is a $\nu \times \nu$ lower triangular matrix, with zero elements on the diagonal. We are now ready to describe our new formulation of fourth-order central Runge-Kutta scheme. For this work, if $x = x_{j+\frac{1}{2}}$ in (2), we obtain CRK schemes namely

$$\left.\frac{d\bar{u}}{dt}\right|_{x_{j+\frac{1}{2}}} = -\frac{1}{h}[f(u(x_{j+1},t)) - f(u(x_j,t))]. \tag{5}$$

Next, this equation is discretized in time with a Runge-Kutta scheme. Therefore, the updated solution will be given by :

$$\bar{u}^{n+1}_{j+\frac{1}{2}} = \bar{u}^n_{j+\frac{1}{2}} - \lambda \sum_{i=1}^{\nu} b_i Y^{(i)}_{j+\frac{1}{2}}, \tag{6}$$

with:

$$Y^{(i)}_{j+\frac{1}{2}} = f\left(u^{(i)}_{j+1}\right) - f\left(u^{(i)}_j\right), \quad u^{(i)}_j = u^n_j + \lambda \sum_{s=1}^{i} a_{is} K^{(s)}_j, \tag{7}$$

where $K_j^{(i)} = -f'(u_j^{(i)})$, and the coefficients b_i and a_{ij} are given by

$$b = \begin{pmatrix} 1/6 \\ 1/3 \\ 1/3 \\ 1/6 \end{pmatrix}, \quad A = \begin{pmatrix} 0 & 0 & 0 & 0 \\ 1/2 & 0 & 0 & 0 \\ 0 & 1/2 & 0 & 0 \\ 0 & 0 & 1 & 0 \end{pmatrix}.$$

For computing the first expression of the right hand side (6), we use the fourth-order reconstruction of Peer et al. [10]. Then, we put polynomial $P_j^n(x)$ on $I_{x_j} := I_j$ in the form:

$$P_j^n(x) = u_j^n + u_j' \left(\frac{x - x_j}{h} \right) + \frac{1}{2!} u_j'' \left(\frac{x - x_j}{h} \right)^2 + \frac{1}{3!} u_j''' \left(\frac{x - x_j}{h} \right)^3, \quad x \in I_j.$$

Here, $u_j^n, u_j'/h, u_j''/h^2$, and u_j'''/h^3 are the approximate point values and the first, second, and third derivatives of $u(x, t^n)$ at $x = x_j$, which are reconstructed from the cell averages, $\{\bar{u}_j^n\}$. It should be noted that this reconstruction [10] satisfies the following three properties:

- $\mathcal{P}1$ − conservation of cell averages: $\bar{P}_j^n(x)|_{x=x_j} = \bar{u}_j^n$.
- $\mathcal{P}2$ − Accuracy: $w(x, t^n) = u(x, t^n) + \mathcal{O}(h^4)$.
- $\mathcal{P}3$ − Non-oscillatory behavior of $\sum_j P_j^n(x)\chi_j(x)$.

Here $\chi_j(x)$ is the characteristic function of I_j.
In order to guarantee property $\mathcal{P}1$, u_j^n must satisfy

$$u_j^n = \bar{u}_j^n - \frac{u_j''}{24}. \tag{8}$$

Remark. Starting with third-order and higher-order accurate methods, the point values aren't equal with cell averages, $u_j^n \neq \bar{u}_j^n$.

The NT scheme [9] uses a second-order accurate limiter for the numerical derivative u_j' in the form

$$u_j' = \mathbf{MM}\left(\Delta\bar{u}^n_{j-\frac{1}{2}}, \Delta\bar{u}^n_{j+\frac{1}{2}} \right). \tag{9}$$

Here, $\Delta\bar{u}^n_{j+\frac{1}{2}} = \bar{u}^n_{j+1} - \bar{u}^n_j$ and the MinMod limiter (**MM**) is defined by

$$\mathbf{MM}(x_1, x_2, \cdots) = \begin{cases} \min_p\{x_p\} & \text{if } x_p > 0 \ \ \forall p, \\ \max_p\{x_p\} & \text{if } x_p < 0 \ \ \forall p, \\ 0 & \text{otherwise.} \end{cases}$$

We observe that the accuracy of (9) decreases when $\Delta\bar{u}_{j-\frac{1}{2}}\Delta\bar{u}_{j+\frac{1}{2}} < 0 \neq u_j'$. Then, the NT scheme modified the uniform nonoscillatory (UNO) limiter of Harten and Osher [23] by adding second-order differences to (9) to get high accuracy,

$$u_j' = \mathbf{MM}\left(\Delta\bar{u}^n_{j-\frac{1}{2}} + \frac{1}{2}\mathbf{MM}\left(\Delta^2\bar{u}^n_{j-1}, \Delta^2\bar{u}^n_j\right), \ \Delta\bar{u}^n_{j+\frac{1}{2}} - \frac{1}{2}\mathbf{MM}\left(\Delta^2\bar{u}^n_j, \Delta^2\bar{u}^n_{j+1}\right) \right), \tag{10}$$

where $\Delta^2\bar{u}^n_j = \Delta\bar{u}^n_{j+\frac{1}{2}} - \Delta\bar{u}^n_{j-\frac{1}{2}}$.

To satisfy properties $\mathcal{P}2 - \mathcal{P}3$, we use the modified UNO limiter of [24]. Similar to the numerical derivative (9), u'''_j depends on its two neighboring third-order differences

$$u'''_j = \mathbf{MM}\left(\Delta^3 \bar{u}^n_{j-\frac{1}{2}}, \Delta^3 \bar{u}^n_{j+\frac{1}{2}}\right), \tag{11}$$

where $\Delta^3 \bar{u}^n_{j+\frac{1}{2}} = \Delta^2 \bar{u}^n_{j+1} - \Delta^2 \bar{u}^n_j$. For obtaining fourth-order accurate approximations of the first derivative, put

$$u'_j = \mathbf{MM}\left(\Delta \bar{u}^n_{j-\frac{1}{2}} + \frac{1}{2}\mathbf{MM}\left(\Delta^2 \bar{u}^n_{j-1} + \frac{7}{12}u'''_{j-1}, \Delta^2 \bar{u}^n_j - \frac{5}{12}u'''_j\right),\right.$$
$$\left.\Delta \bar{u}^n_{j+\frac{1}{2}} - \frac{1}{2}\mathbf{MM}\left(\Delta^2 \bar{u}^n_j + \frac{5}{12}u'''_j, \Delta^2 \bar{u}^n_{j+1} - \frac{7}{12}u'''_{j+1}\right)\right), \tag{12}$$

for further details see [10, 24]. Also, in order to approximate the point values u^n_j of (8) from the cell averages $\{\bar{u}^n_j\}$, we put

$$u''_j = \mathbf{MM}\big(\Delta^2 \bar{u}^n_{j-1} + u'''_{j-1}, \Delta^2 \bar{u}^n_j, \Delta^2 \bar{u}^n_{j+1} - u'''_{j+1}\big). \tag{13}$$

Then the staggered cell averages $\bar{u}^n_{j+\frac{1}{2}}$ are given by

$$\bar{u}^n_{j+\frac{1}{2}} = \frac{1}{2}\big(\bar{u}^n_j + \bar{u}^n_{j+1}\big) - \frac{1}{8}\big(u'_{j+1} - u'_j\big) - \frac{1}{384}\big(u'''_{j+1} - u'''_j\big). \tag{14}$$

Also, to compute the second expression of right hand side (6) we need to approximate f'_j. For this purpose, similar to (7) by combining high-order differences of f put

$$f'_j = \mathbf{MM}\left(\Delta f_{j-\frac{1}{2}} + \frac{1}{2}\mathbf{MM}\left(\Delta^2 f_{j-1} + \frac{2}{3}f'''_{j-1}, \Delta^2 f_j - \frac{1}{3}f'''_j\right),\right.$$
$$\left.\Delta f_{j+\frac{1}{2}} - \frac{1}{2}\mathbf{MM}\left(\Delta^2 f_j + \frac{1}{3}f'''_j, \Delta^2 f_{j+1} - \frac{2}{3}f'''_{j+1}\right)\right), \tag{15}$$

where

$$f'''_j = \mathbf{MM}\left(\Delta^3 f_{j-\frac{1}{2}}, \Delta^3 f_{j+\frac{1}{2}}\right),$$

for further details see [10].

Our scheme is summarized in the following algorithm : Assuming that the cell averages $\{\bar{u}^n_j\}$ are known, we look for the cell averages at the next time step t^{n+1}.

Step 1. Compute the numerical derivatives u'''_j, u''_j, u'_j given by (11), (13), and (12), respectively.

Step 2. Compute the point values u^n_j with (8).

Step 3. Use the results of Step 2 to compute the $u^{(i)}_j$ with (7) and (15).

Step 4. Compute the staggered cell averages at time t^{n+1} according to (6),

$$\bar{u}^{n+1}_{j+\frac{1}{2}} = \frac{1}{2}\big(\bar{u}^n_j + \bar{u}^n_{j+1}\big) - (g_{j+1} - g_j), \tag{16}$$

where the modified numerical flux g_j is obtained by

$$g_j = \frac{1}{8}u'_j + \frac{1}{384}u'''_j + \frac{\lambda}{6}\left(f\left(u_j^{(1)}\right) + 2f\left(u_j^{(2)}\right) + 2f\left(u_j^{(3)}\right) + f\left(u_j^{(4)}\right)\right). \tag{17}$$

IV. STABILITY ANALYSIS

In this section, we report a linear stability analysis, similar to that carried out in [10, 22]. In this work, we use the notation CRKS4 for the Eqs. (16) and (17). To obtain its critical Courant number [25], we apply it to the linear advection equation:

$$u_t + u_x = 0.$$

Thus the scheme will take the form

$$\begin{aligned}
\bar{u}^{n+1}_{j+\frac{1}{2}} &= \bar{u}^n_{j+\frac{1}{2}} - \frac{\lambda}{6}Y^{(1)}_{j+\frac{1}{2}} - \frac{\lambda}{3}Y^{(2)}_{j+\frac{1}{2}} - \frac{\lambda}{3}Y^{(3)}_{j+\frac{1}{2}} - \frac{\lambda}{6}Y^{(4)}_{j+\frac{1}{2}} \\
&= \bar{u}^n_{j+\frac{1}{2}} + \frac{\lambda}{24}\left(u''_{j+1} - u''_j\right) - \lambda\left(\bar{u}^n_{j+1} - \bar{u}^n_j\right) - \frac{\lambda^2}{6}\sum_{i=1}^{3}\left(K^{(i)}_{j+1} - K^{(i)}_j\right), \\
K^{(i)}_j &= -\left(u^n_j + \lambda\sum_{l=1}^{i} a_{i,l}K^{(l)}_j\right)', \quad i = 1, 2, 3.
\end{aligned}$$

Then we can express CRKS4 in terms of cell averages only. We would like to study the linear stability of CRKS4 with a fixed stencil. The amplification factor is obtained by computing the evolution of the initial data: $\bar{u}^n_j = \rho^n e^{ij\xi}$, where $i^2 = -1$. By substituting such expression in CRKS4 for the linear advection equation, we obtain

$$\bar{u}^{n+1}_{j+\frac{1}{2}} = \rho_\lambda(\xi)e^{i\xi/2}\bar{u}^n_j, \quad \xi \in [0, 2\pi].$$

The stability of the scheme can be studied by analyzing the function

$$P_\lambda(\xi) = |\rho_\lambda(\xi)|^2.$$

Let λ^* be the maximum value of λ for which $\max_{0\le\xi\le2\pi} P_\lambda(\xi) \le 1$. The CRKS4 scheme is called stable if $\lambda^* > 0$ exists.

Stencils $(j-3, j-2, j-1, j)$ and $(j, j+1, j+2, j+3)$ are seldom occurred in CRKS4, so we ignore to study stability region for these stencils. Therefore, there are two possibilities for u'''_j, u''_j, u'_j, and f'_j that is,

u'''_j	u''_j	u'_j	f'_j
$\Delta^3\bar{u}^n_{j-\frac{1}{2}}$	$\Delta^2\bar{u}^n_j$	$\Delta\bar{u}^n_{j-\frac{1}{2}} + \frac{1}{2}\left(\Delta^2\bar{u}^n_j - \frac{5}{12}\Delta^3\bar{u}^n_{j-\frac{1}{2}}\right)$	$\Delta f_{j-\frac{1}{2}} + \frac{1}{2}\left(\Delta^2 f_j - \frac{1}{3}\Delta^3 f_{j-\frac{1}{2}}\right)$
$\Delta^3\bar{u}^n_{j+\frac{1}{2}}$	$\Delta^2\bar{u}^n_j$	$\Delta\bar{u}^n_{j+\frac{1}{2}} - \frac{1}{2}\left(\Delta^2\bar{u}^n_j + \frac{5}{12}\Delta^3\bar{u}^n_{j+\frac{1}{2}}\right)$	$\Delta f_{j+\frac{1}{2}} - \frac{1}{2}\left(\Delta^2 f_j + \frac{1}{3}\Delta^3 f_{j+\frac{1}{2}}\right)$

In the first state, we obtain $\lambda^* = 0.4015$ while in the second case we obtain $\lambda^* = 0.4476$. Then we choose the critical Courant number as $\lambda_{\max} = 0.4015$ which satisfies the two states. It

TABLE I. Errors and orders of convergence for Test 1.

N	L_1 error	L_1 order	L_∞ error	L_∞ order
CRKS4 scheme				
40	0.9981 (−3)	–	0.1492 (−2)	–
80	0.7281 (−4)	3.7770	0.1697 (−3)	3.1360
160	0.4996 (−5)	3.8652	0.1891 (−4)	3.1658
320	0.3553 (−6)	3.8135	0.2094 (−5)	3.1747
640	0.2042 (−7)	4.1211	0.2308 (−6)	3.1813
CNO4 scheme				
40	0.1371 (−2)	–	0.1986 (−2)	–
80	0.9730 (−4)	3.8161	0.2239 (−3)	3.1490
160	0.6912 (−5)	3.8152	0.2512 (−4)	3.1562
320	0.4695 (−6)	3.8801	0.2792 (−5)	3.1696
640	0.3135 (−7)	3.9043	0.3088 (−6)	3.1764

should be noted that CRKS4 allows a larger Courant number than CNO4 [10] , $\lambda_{\max} = 0.3408$, while both methods use similar stencils. Also, the stability restriction of CRK-WENO(Weighted Essentially Nonoscillatory) [19] is less restrictive than CRKS4. We refer the interested reader to references [26–30] for more useful research works on the subject of the current paper.

V. NUMERICAL RESULTS

A. Scalar Test Problems

In this subsection, we describe the results of numerical experiments using some Scalar test problems with periodic boundary conditions. Also we compare results with CNO4 [10]. It should be noted that in Figures 1–9, results obtained using the methods of CRKS4, CNO4, and exact or reference solution are shown by '×', '.' and solid line respectively.

Test 1. We start with linear advection equation $u_t + u_x = 0$, over the long time interval $T = 10$, with the smooth initial condition $u(x, 0) = \sin(\pi x)$. This test is used to check the convergence rate. We solve the test with $\lambda = 0.9\lambda_{\max}$ and $x \in [-1, 1]$. The L_1 and L_∞ errors and orders of convergence by CRKS4 and CNO4 are shown in Table I. We see that both CRKS4 and CNO4 converge to fourth-order in L_1 as the computational grid is refined. But, comparing the magnitude of errors produced by CRKS4 and CNO4 for this test problem shows that CRKS4 performs better.

Test 2. In this test, we consider linear advection equation $u_t + u_x = 0$, over the time interval $T = 4$, with the initial condition $u(x, 0) = 1$ for $|x| < \frac{1}{3}$ and $u(x, 0) = 0$ elsewhere. In this test problem, we put $\lambda = 0.9\lambda_{\max}$ and $x \in [-1, 1]$. The L_1 and L_∞ errors by CRKS4 and CNO4 are reported in Table II. Our results show CRKS4 yields better accuracy in L_1 than CNO4, but results of errors obtained in L_∞ by CRKS4 and CNO4 are comparable.

TABLE II. Errors for approximation of Test 2 at $T = 4$.

	CRKS4 scheme		CNO4 scheme	
N	L_1 error	L_∞ error	L_1 error	L_∞ error
25	0.1706	0.3876	0.1903	0.3870
50	0.9710 (−1)	0.4124	0.1102	0.4068
100	0.5486 (−1)	0.4359	0.6477 (−1)	0.4246
200	0.2786 (−1)	0.4226	0.3801 (−1)	0.4395

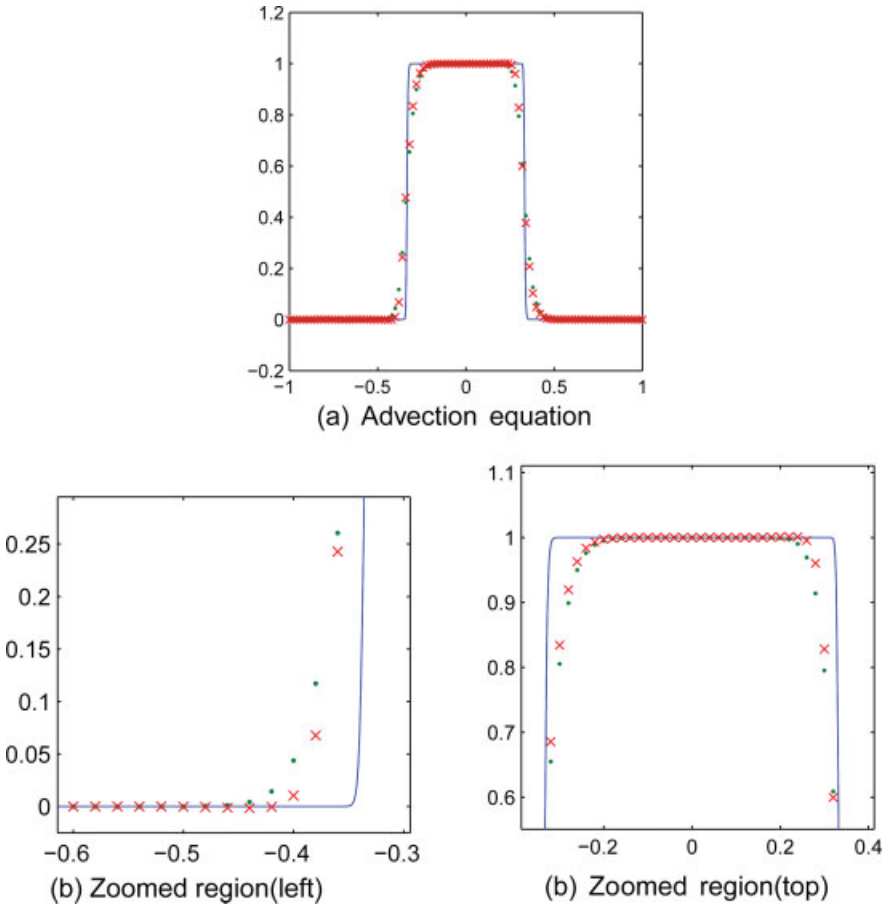

FIG. 1. Test 2 by $N = 100$ at $T = 4$. CRKS4 "×", CNO4 ".". [Color figure can be viewed in the online issue, which is available at wileyonlinelibrary.com.]

The approximations at $T = 4$ on 100 cells are shown in Fig. 1. We note that CRKS4 gives an overall better solution than CNO4.

Test 3. For the third test problem, we consider the in-viscid Burgers' equation $u_t + (0.5u^2)_x = 0$, with the initial condition $u(x, 0) = 1 + 0.5\sin(\pi x)$ and $\lambda = \frac{2}{3}\lambda_{\max}$. It is known that the unique entropy solution of the problem develops a shock discontinuity at $T_s = 2/\pi \simeq 0.7$. In Table III, we present the errors by CRKS4 and CNO4 after the shock ($T = 1.5$). Comparing the magnitude

TABLE III. Errors of Burgers' equation for Test 3 at $T = 1.5$ (after shock).

	CRKS4		CNO4	
N	L_1 error	L_∞ error	L_1 error	L_∞ error
40	0.6287 (−2)	0.5010 (−1)	0.6776 (−2)	0.6023 (−1)
80	0.2859 (−2)	0.5168 (−1)	0.3211 (−2)	0.6179 (−1)
160	0.1368 (−2)	0.5074 (−1)	0.1588 (−2)	0.6150 (−1)
320	0.6490 (−3)	0.4720 (−1)	0.7833 (−3)	0.6048 (−1)

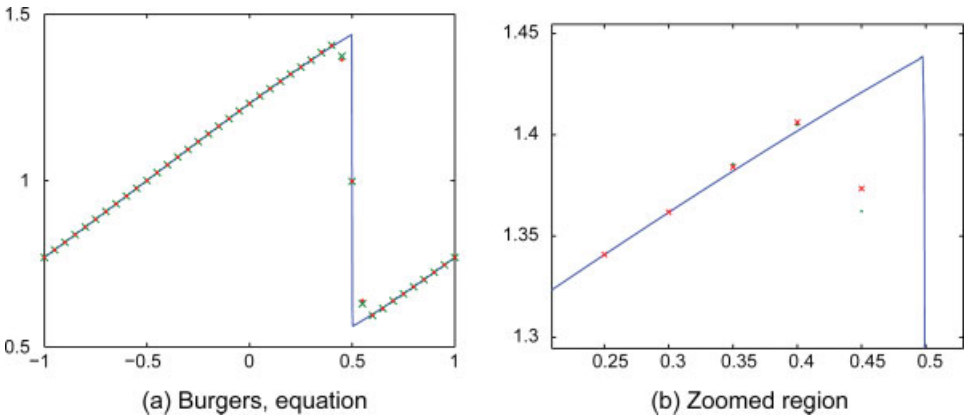

FIG. 2. Test 3 by $N = 40$ at $T = 1.5$. CRKS4 "×", CNO4 ".". [Color figure can be viewed in the online issue, which is available at wileyonlinelibrary.com.]

of errors by CRKS4 and CNO4 schemes for this test problem shows that the CRKS4 yields better accuracy in both L_1 and L_∞ norms when $T = 1.5$ (after shock). We end this test with the different approximations on 40 cells in Fig. 2. We observe that CRKS4 is sharper than CNO4 when resolving the shock.

Test 4. In this test problem, we solve the in-viscid Burgers' equation $u_t + (0.5u^2)_x = 0$, with the initial condition $u(x, 0) = 1$ for $|x| < \frac{1}{3}$ and elsewhere $u(x, 0) = 0$. In this test problem we set $\lambda = \frac{2}{3}\lambda_{\max}$. In Table IV, we show the corresponding errors for the respective number of cells and we note that CRKS4 gives better accuracy than CNO4 in both L_1 and L_∞ norms. In Fig. 3, we display the different approximations on 80 cells. We see that CRKS4 is sharper than CNO4 on the shock.

B. Hyperbolic Systems of Equations

In this subsection, we test CRKS4 and CNO4 schemes on the system of Euler equations for a polytropic gas, with $\gamma = 1.4$,

$$\frac{\partial}{\partial t}\begin{pmatrix}\rho\\ \rho q\\ E\end{pmatrix} + \frac{\partial}{\partial x}\begin{pmatrix}\rho q\\ \rho q^2 + p\\ q(E+p)\end{pmatrix} = 0, \quad p = (\gamma - 1)\left(E - \frac{1}{2}\rho q^2\right). \tag{18}$$

Here, ρ, q, p, and E are the density, velocity, pressure, and total energy of the conserved fluid, respectively. There are two recipes to extend the numerical schemes for solving hyperbolic systems of conservation laws. The first approach is componentwise extension, also, we can utilize

TABLE IV. Errors of Burgers' equation for Test 4 at $T = 0.64$.

	CRKS4		CNO4	
N	L_1 error	L_∞ error	L_1 error	L_∞ error
40	0.4699 (−1)	0.4626	0.5857 (−1)	0.5608
80	0.2328 (−1)	0.4133	0.2407 (−1)	0.3273
160	0.1127 (−1)	0.3331	0.1267 (−1)	0.4399
320	0.5496 (−2)	0.2021	0.5983 (−2)	0.3217

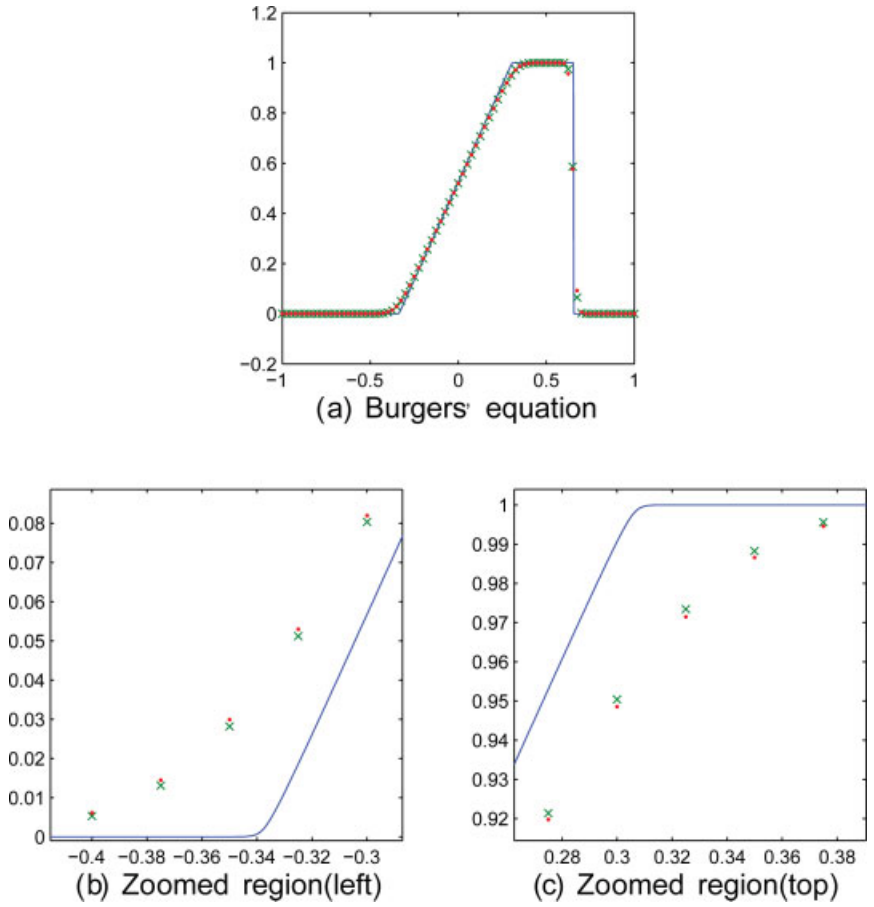

FIG. 3. Test 4 by $N = 80$ at $T = 0.64$. CRKS4 "×", CNO4 ".". [Color figure can be viewed in the online issue, which is available at wileyonlinelibrary.com.]

characteristic decomposition. In this work, we use the first approach which is less costly (because we do not need the Jacobian matrix $A(u) := \frac{\partial f}{\partial u}$ and eigenstructure of the system). We choose the time step dynamically with CFL restriction

$$\Delta t = \frac{0.9\lambda_{\max} h}{\max_j (c_j + |q_j|)},$$

where c_j and q_j are the local sound speed and velocity, respectively. This time step evaluation technique can accommodate for problems where the characteristic speeds change wildly in time.

Test 5 (Sod's Problem)**.** In this test which is taken from [31], we solve (18) with the initial condition:

$$u(x,0) = \begin{cases} (1,0,2.5)^T & 0 \le x < 0.5, \\ (0.125,0,0.25)^T & 0.5 \le x \le 1, \end{cases} \quad x \in [0,1].$$

Figure 4 shows the performance of CRKS4 and CNO4 methods at $T = 0.16$ with $N = 100$. Comparing the results in Fig. 4 we note that the CNO4 scheme is still comparable with CRKS4

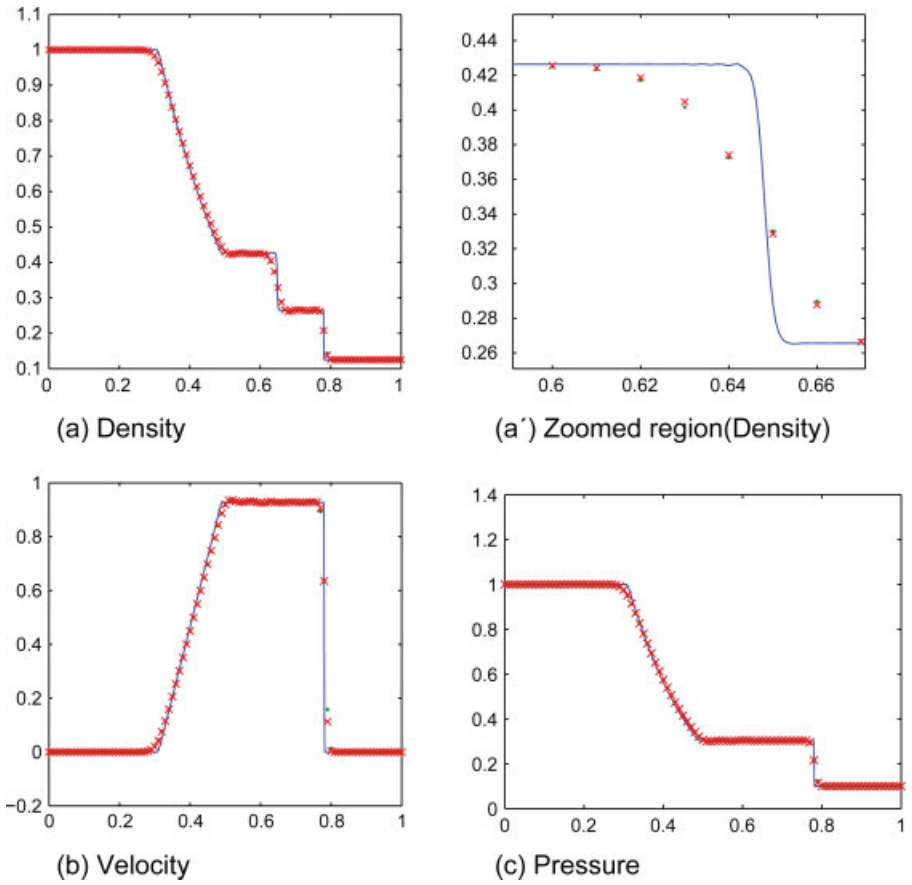

FIG. 4. Test 5 by $N = 100$ at $T = 0.16$. CRKS4 "×" CNO4 "." [Color figure can be viewed in the online issue, which is available at wileyonlinelibrary.com.]

scheme. But the CRKS4 scheme gives better resolution at the two ends of the rarefaction wave, the contact and the shock.

Test 6 (Lax's Problem)**.** In this test which is taken from [32] we solve (18) with the initial condition:

$$u(x,0) = \begin{cases} (0.445, 0.31061, 8.92840289)^T & 0 \le x < 0.5, \\ (0.5, 0, 1.4275)^T & 0.5 \le x \le 1, \end{cases} \quad x \in [0,1],$$

For this more difficult shock tube problem, Fig. 5 shows the performance of CRKS4 and CNO4 schemes at $T = 0.16$ with $N = 100$. Similar to the Sod's test problem, CRKS4 scheme gives better resolution than CNO4 scheme. In Fig. 5 (a') we observe that CRKS4 is sharper than CNO4 in particular for the density profile of this Riemann test problem. Also, we observe that there are oscillations even in the reference solution. It should be noted that these oscillations are due to the fact that there is a lack of characteristic information, for further details see [19].

Test 7 (Shock-Entrop Problem)**.** In this test which is used by authors of [33], we solve the Euler equations (18) with a moving Mach = 3 shock interacting with sine waves in density, that is,

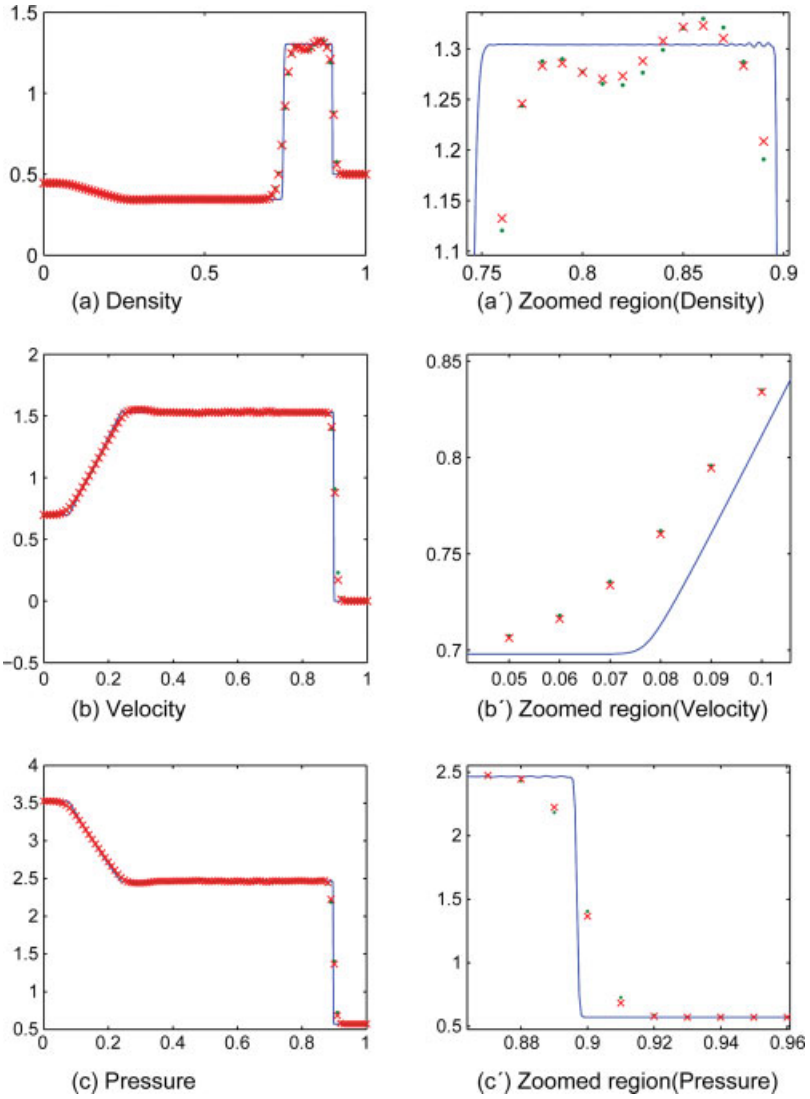

FIG. 5. Test 6 by $N = 100$ at $T = 0.16$. CRKS4 "×" CNO4 "." [Color figure can be viewed in the online issue, which is available at wileyonlinelibrary.com.]

$$u(x,0) = \begin{cases} (3.85714, 10.1418096304, 39.16655928489427)^T & -5 \le x < -4, \\ (1 + 0.2\sin(5x), 0, 2.5)^T & -4 \le x \le 5, \end{cases} \quad x \in [-5, 5].$$

The flow contains physical oscillations which have to be resolved by the numerical methods(CRKS4 and CNO4 schemes). The "reference solution," which is a converged solution computed by CNO4 with 2000 grid points. We test the performance of the CRKS4 and CNO4 methods in smooth regions and the ability to capture shocks with $N = 200$. We show the numerical solutions of the density profile in Fig. 6 at $T = 1.8$. We observe that CRKS4 gives better resolution than CNO4.

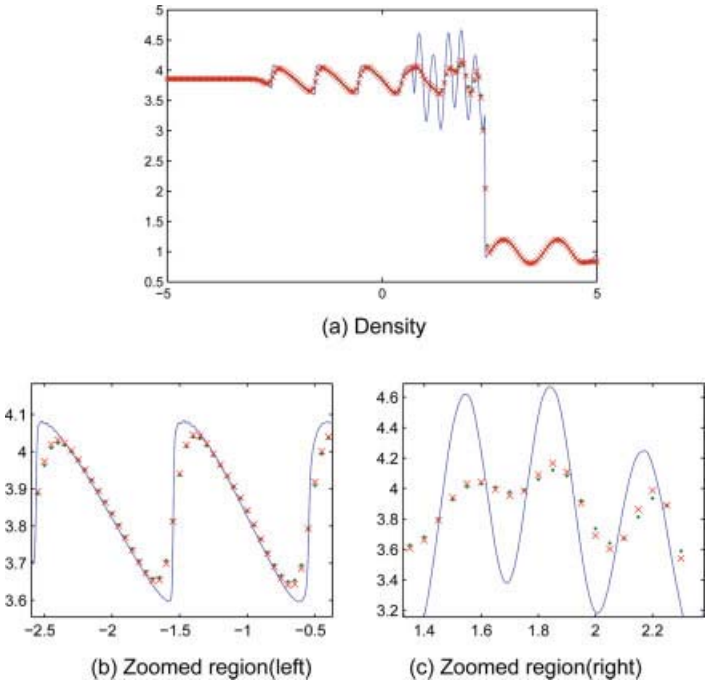

FIG. 6. Test 7 by $N = 200$ at $T = 1.8$. CRKS4 "$\times$", CNO4 ".". [Color figure can be viewed in the online issue, which is available at wileyonlinelibrary.com.]

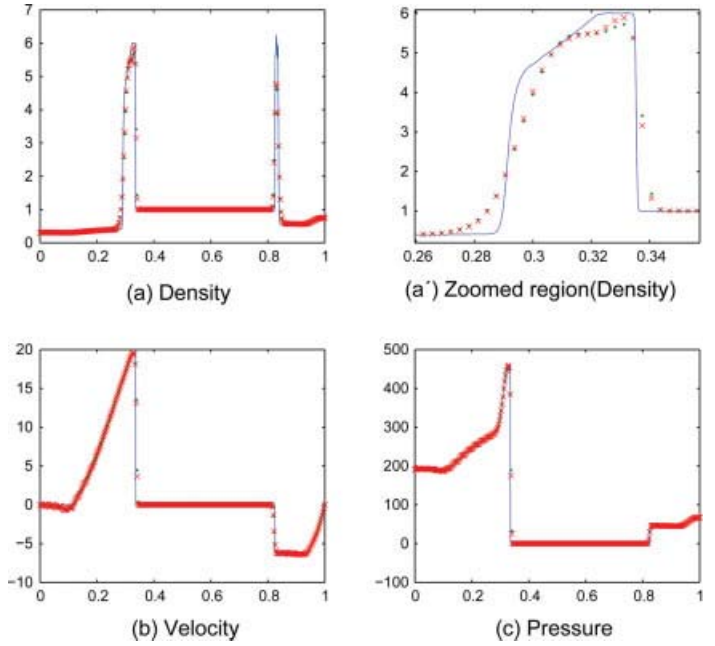

FIG. 7. Test 8 by $N = 320$ at $T = 0.01$. CRKS4 "$\times$" CNO4".". [Color figure can be viewed in the online issue, which is available at wileyonlinelibrary.com.]

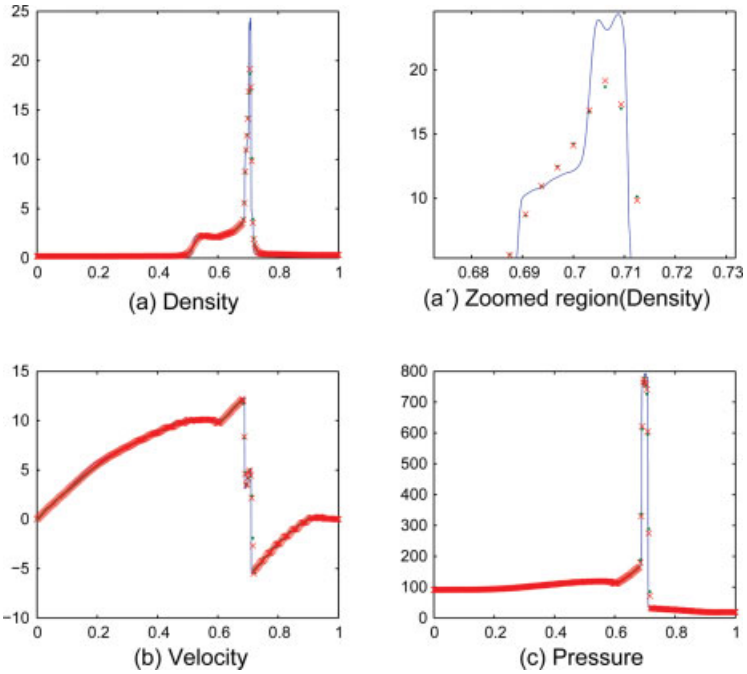

FIG. 8. Test 8 by $N = 320$ at $T = 0.03$. CRKS4 "×" CNO4 "." [Color figure can be viewed in the online issue, which is available at wileyonlinelibrary.com.]

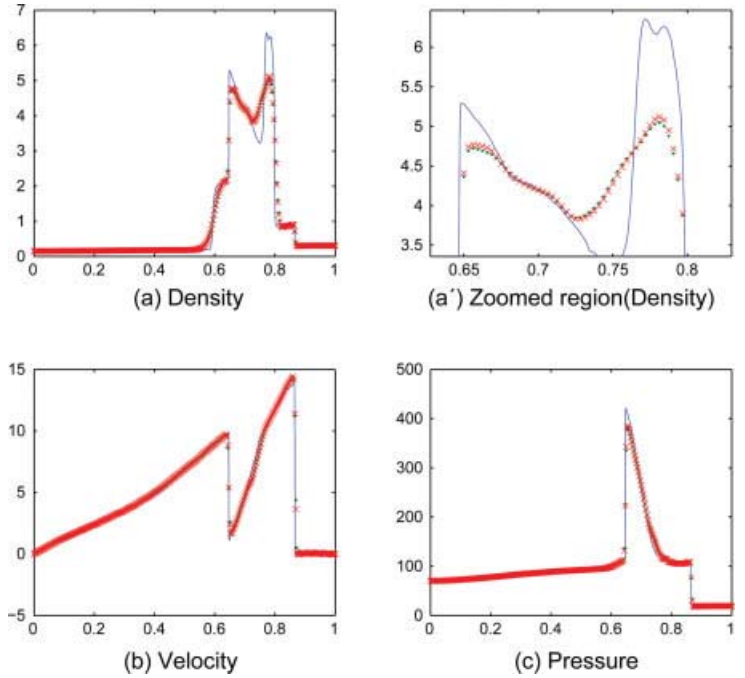

FIG. 9. Test 8 by $N = 320$ at $T = 0.038$. CRKS4 "×" CNO4 "." [Color figure can be viewed in the online issue, which is available at wileyonlinelibrary.com.]

Test 8 (Woodward and Colella's Problem)**.** For the final test which is taken from [34], we solve the Euler equations (18) with a shock interaction problem with solid wall boundary conditions, applied to both ends given by the initial data

$$u(x,0) = \begin{cases} (1,0,2500)^T & 0 \le x < 0.1, \\ (1,0,0.025)^T & 0.1 \le x < 0.9, \\ (1,0,250)^T & 0.9 \le x \le 1, \end{cases} \quad x \in [0,1],$$

$$\text{Integration times are: } T = 0.01, \quad T = 0.03, \quad T = 0.038.$$

The computations are done, using $N = 320$, and the solution is displayed together with a "reference solution," obtained by the CNO4 scheme with $N = 2560$. In Fig. 7, we show the density, the velocity, and the pressure at $T = 0.01$. We observe in the zoomed regions of the density profile that CRKS4 gives better resolution than CNO4. Also we plot the numerical results of the above problem in Figs. 8 and 9 at time $T = 0.03$ and $T = 0.038$, respectively. We note that the CRKS4 gives better resolution than CNO4.

VI. CONCLUSION

In this article, we have introduced a new fourth-order central Runge-Kutta scheme. For that, we used the fourth-order reconstruction of Peer et al. [10] and a Runge-Kutta procedure. Numerical results on scalar test problem show that this scheme resolves discontinuities sharply while avoiding oscillations. In comparison with the fourth-order central nonoscillatory scheme [10], we saw that the fourth-order central Runge-Kutta method gives better resolution. The new fourth-order central Runge-Kutta technique was extended to solve hyperbolic systems of conservation laws using a componentwise extension. Then we solved the Euler equations of gas dynamics, and we observed that the proposed scheme gives better resolution than the fourth-order central nonoscillatory method.

The authors would like to thank A. A. I. Peer for his valuable programming advice. The authors are very grateful to the three reviewers for carefully reading the paper and for their comments.

References

1. M. Simpson and K. Landman, Nonmonotone chemotactic invasion: high-resolution simulation, phase plane analysis and new benchmark problems, J Comput Phys 225 (2007), 6–12.
2. G. Russo, Central schemes for conservation laws with application to shallow water equations, in Trends and applications of mathematics to mechanics: STAMM 2002, Springer-Verlag, Italia SRL, 2005, pp. 225–246.
3. E. Gabetta, L. Pareschi, and M. Ronconi, Central schemes for hydrodynamical limits of discrete-velocity kinetic models, Trans Theo Stat Phys 29 (2000), 465–477.
4. J. Balbas and E. Tadmor, Non-oscillatory central schemes for one-and two-dimensional MHD equations. II: High-order semi-discrete schemes, SIAM J Sci Comput 28 (2006), 533–560.
5. M. Dehghan, Finite difference procedures for solving a problem arising in modeling and design of certain optoelectronic devices, Mathematics Comput Simul 71 (2006), 16–30.
6. M. Dehghan, On the solution of an initial-boundary value problem that combines Neumann and integral condition for the wave equation, Numer Methods Partial Differential Eq 21 (2005), 24–40.

7. R. J. LeVeque, Finite volume methods for hyperbolic problems, Cambridge Texts in Applied Mathematics, Cambridge University Press, Cambridge, UK, 2002.
8. X. D. Liu and E. Tadmor, Third order nonoscillatory central scheme for hyperbolic conservation laws, Numer Math 79 (1998), 379–425.
9. H. Nessyahu and E. Tadmor, Non-oscillatory central differencing for hyperbolic conservation laws, J Comput Phys 87 (1990), 408–463.
10. A. A. I. Peer, A. Gopaul, M. Z. Dauhoo, and M. Bhuruth, A new fourth-order non-oscillatory central scheme for hyperbolic conservation laws, Appl Numer Math 58 (2008), 674–688.
11. S. K. Godunov, A finite difference method for the numerical computation of discontinuous solutions of the equations of fluid dynamics, Math Sb 47 (1959), 271–290.
12. K. O. Friedrichs and P. D. Lax, Systems of conservation equations with a convex extension, Proc Nat Acad Sci 68 (1971), 1686–1688.
13. G. S. Jiang and E. Tadmor, Nonoscillatory central schemes for multidimensional hyperbolic conservation laws, SIAM J Sci Comput 19 (1998), 1892–1917.
14. X. D. Liu and S. Osher, Non-oscillatory high order accurate self-similar maximum principle satisfying shock capturing schemes I, SIAM J Numer Anal 33 (1996), 760–779.
15. V. Romano and G. Russo, Numerical solution for hydrodynamical models of semiconductors, Math Models Methods Appl Sci 10 (2000), 1099–1120.
16. L. Pareschi, Central differencing based numerical schemes for hyperbolic conservation laws with relaxation terms, SIAM J Numer Anal 39 (2001), 1395–1417.
17. S. F. Liotta, V. Romano, and G. Russo, Central schemes for balance laws of relaxation type, SIAM J Numer Anal 38 (2000), 1337–1356.
18. S. Bryson and D. Levy, High-order semi-discrete central-upwind schemes for multi-dimensional Hamilton-Jacobi equations, J Comput Phys 189 (2003), 63–87.
19. L. Pareschi, G. Puppo, and G. Russo, Central Runge Kutta schemes for conservation laws, SIAM J Sci Comput 26 (2005), 979–999.
20. M. Zennaro, Natural continuous extensions of Runge-Kutta methods, Math Comp 46 (1986), 119–133.
21. A. Kurganov, S. Noelle, and G. Petrova, Semi-discrete central-upwind schemes for hyperbolic conservation laws and Hamilton-Jacobi equations, SIAM J Sci Comput 23 (2001), 707–740.
22. F. Bianco, G. Puppo, and G. Russo, High-order central schemes for hyperbolic systems of conservation laws, SIAM J Sci Comput 21 (1999), 294–322.
23. A. Harten and S. Osher, Uniformly high-order accurate nonoscillatory schemes, I, SIAM J Numer Anal 24 (1987), 279–309.
24. A. A. I. Peer, A. Gopaul, M. Z. Dauhoo, and M. Bhuruth, New high-order ENO reconstruction for hyperbolic conservation laws, Proceedings of the International Conference on Computational and Mathematical Methods in Science and Engineering, CMMSE-2005 Alicante, June 27–30, 2005, pp. 446–455.
25. J. C. Strikwerda, Finite difference schemes and partial differential equations, SIAM, 2004.
26. A. Kurganov and G. Petrova, A third-order semidiscrete genuinely multidimensional central scheme for hyperbolic conservation laws and related problems, Numer Math 88 (2001), 683–729.
27. A. Kurganov and E. Tadmor, New high-resolution central schemes for non-linear conservation laws and convection-diffusion equations, J Comput Phys 160 (2000), 241–282.
28. D. Levy, G. Puppo, and G. Russo, Central WENO schemes for hyperbolic systems of conservation laws, Math Model Numer Anal 33 (1999), 547–571.
29. D. Levy, G. Puppo, and G. Russo, A fourth-order central WENO schemes for multidimensional hyperbolic systems of conservation laws, SIAM J Sci Comput 24 (2002), 456–480.

30. D. Levy, G. Puppo, and G. Russo, Compact central WENO schemes for multidimensional conservation laws, SIAM J Sci Comput 22 (2000), 656–672.

31. G. Sod, A survey of several finite difference methods for systems of non-linear hyperbolic conservation laws, J Comput Phys 27 (1978), 1–31.

32. P. D. Lax, Weak solutions of non-linear hyperbolic equations and their numerical computation, Comm Pure Appl Math 7 (1954), 159–193.

33. C. W. Shu and S. Osher, Efficient implementation of essentially non-oscillatory shock-capturing schemes II, J Comput Phys 83 (1989), 32–78.

34. P. Woodward and P. Clella, The numerical solution of two-dimensional fluid flow with strong shocks, J Comput Phys 54 (1988), 115–173.